Article

Intracellular pH controls WNT downstream of glycolysis in amniote embryos

https://doi.org/10.1038/s41586-020-2428-0

Received: 10 January 2019

Accepted: 2 April 2020

Published online: 24 June 2020

Check for updates

Masayuki Oginuma[1,2,3,6], Yukiko Harima[1,2,6], Oscar A. Tarazona[1,2], Margarete Diaz-Cuadros[1,2], Arthur Michaut[1,2], Tohru Ishitani[3,4], Fengzhu Xiong[1,2] & Olivier Pourquié[1,2,5]✉

Formation of the body of vertebrate embryos proceeds sequentially by posterior addition of tissues from the tail bud. Cells of the tail bud and the posterior presomitic mesoderm, which control posterior elongation[1], exhibit a high level of aerobic glycolysis that is reminiscent of the metabolic status of cancer cells experiencing the Warburg effect[2,3]. Glycolytic activity downstream of fibroblast growth factor controls WNT signalling in the tail bud[3]. In the neuromesodermal precursors of the tail bud[4], WNT signalling promotes the mesodermal fate that is required for sustained axial elongation, at the expense of the neural fate[3,5]. How glycolysis regulates WNT signalling in the tail bud is currently unknown. Here we used chicken embryos and human tail bud-like cells differentiated in vitro from induced pluripotent stem cells to show that these cells exhibit an inverted pH gradient, with the extracellular pH lower than the intracellular pH, as observed in cancer cells[6]. Our data suggest that glycolysis increases extrusion of lactate coupled to protons via the monocarboxylate symporters. This contributes to elevating the intracellular pH in these cells, which creates a favourable chemical environment for non-enzymatic β-catenin acetylation downstream of WNT signalling. As acetylated β-catenin promotes mesodermal rather than neural fate[7], this ultimately leads to activation of mesodermal transcriptional WNT targets and specification of the paraxial mesoderm in tail bud precursors. Our work supports the notion that some tumour cells reactivate a developmental metabolic programme.

In differentiated adult cells, the intracellular pH (pHi) is around 7.2, whereas the extracellular pH (pHe) is around 7.4. In most cancer cells, the regulation of pHe and pHi is significantly different from normal cells: whereas the pHe is lower (6.7–7.1) than in normal adult cells, the pHi is higher (>7.4)[8]. To examine whether the presomitic mesoderm (PSM) and tail bud cells also exhibit an inverted pHe–pHi gradient, we electroporated the ratiometric pH sensor pHluorin[9,10] in the anterior primitive streak region (which contains the PSM precursors) of stage-4 Hamburger and Hamilton (HH) chicken embryos[11]. One day after electroporation, embryos were incubated in buffers of different pH (pH 5.5, pH 6.5 and pH 7.5) with the protonophores nigericin and valinomycin to equilibrate the pHi to the buffer pH[10]. The 488/405-nm ratio in the tail bud and the PSM decreased as the buffer pH increased (Extended Data Fig. 1a, b). We next measured the 488/405-nm ratio in electroporated embryos without protonophores. We observed a posterior–anterior gradient of the pHluorin 488/405-nm signal ratio in most wild-type embryos ($n = 11$ of 13) (Fig. 1a, b). Tail bud cells show a lower 488/405-nm ratio (higher pHi), whereas anterior PSM cells show a higher ratio (lower pHi) (Fig. 1a, b). We also microdissected entire PSMs from two-day-old chicken embryos and incubated them with the ratiometric pH-sensitive dye BCECF. Variations of the fluorescence ratio along the PSM confirmed the existence of a pHi gradient (Extended Data Fig. 1c, d). Thus, anterior PSM cells have higher intracellular acidity than posterior cells.

Treating embryos electroporated with pHluorin in the PSM with the glycolysis inhibitor 2-deoxy-D-glucose (2DG) ex ovo increased the overall 488/405-nm ratio of the tail bud and the posterior PSM (Fig. 1c), suggesting a decrease in the pHi. A majority of electroporated embryos grown on 2DG plates show no anterior–posterior pHi gradient compared to control embryos (Fig. 1d). Culturing 2-day-old chicken embryos in agar plates containing only PBS and 8.3 mM glucose at pH 7.2 can sustain normal development[3] (Fig. 1e). Decreasing the glucose concentration to 0.83 mM and 0 mM resulted in a dose-dependent slowing down of axis elongation and a decrease in the pHi, as observed with 2DG treatment[3] (Fig. 1e, f, Extended Data Fig. 2a, b). Shallower and more variable pHi gradients were evidenced in embryos cultured in low-glucose conditions (Fig. 1g). Thus, decreasing glycolytic activity leads to an increase of intracellular acidity in PSM cells.

When embryos electroporated with pHluorin in minimal medium buffered at different pH were cultured for 3 h, the signal ratio in the posterior PSM increased when the pH of the medium decreased. Thus, exposing embryos to a lower pHe leads to a corresponding acidification of the pHi in the PSM[12–14] (Fig. 1h). When embryos were cultured at pH 6.0 or pH 5.3, axis elongation was significantly slowed down and

[1]Department of Genetics, Harvard Medical School, Boston, MA, USA. [2]Department of Pathology, Brigham and Women's Hospital, Boston, MA, USA. [3]IMCR, Gunma University, Gunma, Japan. [4]RIMD, Osaka University, Osaka, Japan. [5]Harvard Stem Cell Institute, Harvard University, Cambridge, MA, USA. [6]These authors contributed equally: Masayuki Oginuma, Yukiko Harima. ✉e-mail: pourquie@genetics.med.harvard.edu

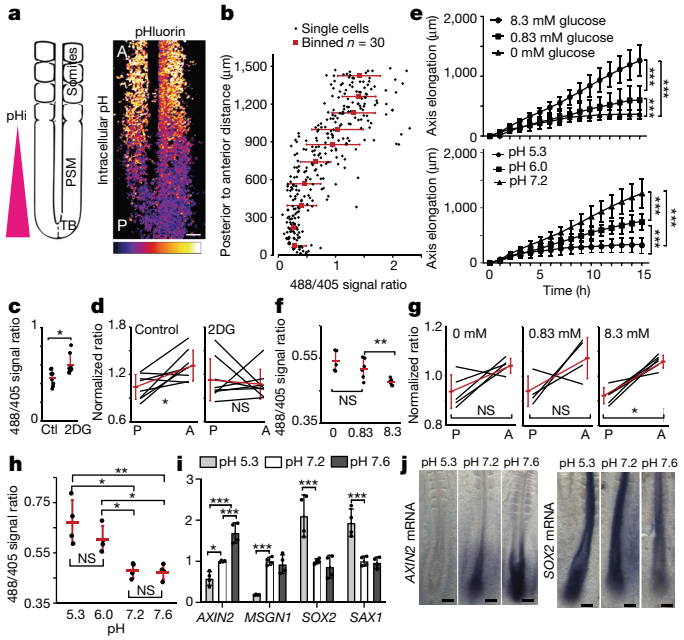

Fig. 1 | A glycolysis-dependent pHi gradient in the tail bud. a, Tail bud (TB) and the PSM region in a two-day-old chicken embryo; the pHi gradient is in pink (left). The corresponding region electroporated with pHluorin ($n = 13$) is also shown (right). The acidic regions are in yellow. A, anterior; P, posterior. **b**, The 488/405-nm ratio in cells in a representative embryo ($n = 3$). **c**, Average 488/405-nm ratio of the PSM region in control (Ctl) ($n = 8$) and 2DG-treated ($n = 8$) embryos. Two-sided, unpaired *t*-test. *$P = 0.01$. **d**, Normalized average 488/405-nm ratio in control ($n = 8$) and 2DG-treated ($n = 8$) embryos. The red lines (and error bars) indicate the mean (±s.d.) of different embryos. Two-sided, paired *t*-tests, *$P = 0.02$; NS (not significant), $P = 0.69$. **e**, Axis elongation in 2-day-old embryos in vitro: (top) pH 7.2, 8.3 mM ($n = 6$), 0.83 mM ($n = 3$) and 0 mM glucose ($n = 6$); (bottom) pH 7.2 ($n = 6$), pH 6.0 ($n = 5$) and pH 5.3 ($n = 8$). Two-way analysis of variance (ANOVA) followed by Tukey's multiple comparison test. ***$P < 0.0005$. **f**, Average 488/405-nm ratio of the PSM region of 2-day-old embryos at pH 7.2 with 8.3 mM ($n = 6$), 0.83 mM ($n = 5$) and 0 mM glucose. Two-sided, unpaired *t*-test. **$P = 0.001$ and NS, $P > 0.05$. **g**, Normalized average 488/405-nm ratio. Embryos were cultured at pH 7.2: 8.3 mM ($n = 6$), 0.83 mM ($n = 5$) and 0 mM glucose ($n = 6$). Compared average ratios ± s.d. (bars of the red line) of pooled samples. Two-sided, paired *t*-test. *$P = 0.002$; NS, $P > 0.05$. **h**, Average 488/405-nm fluorescence ratio of 2-day-old chicken embryos at pH 5.3: $n = 4$, pH 6.0: $n = 4$, pH 7.2: $n = 4$ and pH 7.6: $n = 4$ (two independent experiments). Two-sided, unpaired *t*-test. *$P < 0.01$, **$P < 0.001$ and NS, $P > 0.05$. **i**, *MSGN1*, *SAX1*, *SOX2* and *AXIN2* expression in the posterior region of 2-day-old chicken embryos at different pH ($n = 4$ for each gene). Data were normalized with pH-7.2 samples. Tukey's multiple comparison test. *$P < 0.05$ and ***$P < 0.001$. **j**, Two-day-old chicken embryos hybridized with *AXIN2* (pH 5.3: $n = 6$, pH 7.2: $n = 6$ and pH 7.6: $n = 4$) and *SOX2* (pH 5.3: $n = 6$, pH 7.2: $n = 4$ and pH 7.6: $n = 5$) probes. In **b**–**i**, mean ± s.d. is shown. In **a**, **b** and **j**, ventral views are shown with the anterior to the top. Scale bar, 100 μm. Exact *P* values can be found in the corresponding Source Data files.

rapidly stalled, similar to glycolysis inhibition[3] (Fig. 1e, Extended Data Fig. 2c, d). Embryos that exhibited elongation arrest after exposition to a low-pH buffer resumed normal development when switched back to control medium (Extended Data Fig. 2e). This developmental arrest resembles the reversible growth arrest observed in cancer cells exposed to a lower pHi[6,12,15].

Blocking glycolysis with 2DG in vivo results in most neuromesodermal precursors (NMPs) differentiating to a neural SOX2/SAX1-positive fate, ultimately leading to elongation arrest[3]. Culturing embryos in a low-pH buffer decreases the expression of the WNT target *AXIN2*, whereas high pH results in stronger expression (Fig. 1i, j). A similar behaviour is observed for *MSGN1*, a PSM-specific WNT target[16] (Fig. 1i, Extended Data Fig. 1e). By contrast, the neural genes *SOX2* and *SAX1* showed an opposite behaviour: they were upregulated at low pH (Fig. 1i, j, Extended Data Fig. 1f). Thus, higher pHi favours canonical WNT signalling, which promotes the paraxial mesoderm fate from NMPs, whereas lower pHi inhibits WNT, which promotes the neural fate.

Lactate and protons are extruded from the cell by the lactate/H^+ symporters MCT1/4, which regulate pHi in highly glycolytic tissues[13]. *MCT1* (also known as *SLC16A1*) was expressed in a graded manner in the tail bud and the posterior PSM, paralleling the pHi gradients (Extended Data Fig. 3a). *MCT4* (also known as *SLC16A3*) was also expressed in the chicken and mouse PSM[2,15]. Day-2 chicken embryos treated with the MCT inhibitor α-cyano-4-hydroxycinnamic acid (CNCn) exhibit increased intracellular lactate levels and downregulation of *AXIN2* and *T* (also known as *TBXT*), but upregulation of *SOX2* and *SAX1* (Extended Data Fig. 3b–d). Thus, inhibition of MCT function mimics glycolysis inhibition or decreasing pHi. This suggests a mechanism in which elevated glycolysis leads to increased lactate and proton extrusion via MCT transporters, thus increasing pHi in tail bud cells.

Treatment of human induced pluripotent stem (iPS) cells with the glycogen synthase kinase 3β inhibitor CHIR99021 (Chir) and the bone morphogenetic protein inhibitor LDN193189 (LDN) (CL medium), induces cells to differentiate to a SOX2–brachyury-positive NMP-like fate after day 1[17,18]. After day 2, more than 95% of the cells differentiate to a MSGN1-positive posterior PSM fate[17–19]. We observed a significant decrease of the extracellular acidification rate and glycolytic ATP production (Fig. 2a, b) during in vitro differentiation. In the differentiating iPS cultures, nuclear β-catenin localization (which is generally associated with WNT activation[20]) peaked at day 2[19] (Extended Data Fig. 4a, b). Time-lapse imaging of a human iPS reporter line expressing a β-catenin–GFP fusion differentiating towards the PSM fate confirmed the transient nuclear localization of β-catenin at days 1–2 (Fig. 2c). This was correlated with the expression of the PSM WNT targets *AXIN2*, *TBX6* and *MSGN1*, which peaked around days 2–3 of differentiation[21–23] (Extended Data Fig. 4c–e). Thus, human PSM cells exhibit an increased WNT response during the early phase of PSM maturation in vitro, as observed in the posterior PSM in vivo[24,25]. We next examined the pHi of differentiating human iPS cells using BCECF[10]. We observed a higher pHi (>7.5) at day 2 that progressively decreased in sync with WNT signalling after day 3 (Fig. 2d). Thus, the decrease of glycolytic and WNT activity parallels a progressive decrease of pHi in human PSM cells differentiating in vitro.

Culturing iPS cells in CL medium at different pH could predictably change the pHi of cells within physiological range (Fig. 2e). Decreasing the pHi by culturing cells in acidic conditions at a stage equivalent to the NMP stage increased the expression of *SOX1* and decreased the expression of *AXIN2* (Fig. 2g). A similar phenotype was observed with CNCn (Extended Data Fig. 3e). By contrast, cells exposed to basic conditions (pH 7.5–8) showed a reverse phenotype (Fig. 2g). Thus, higher pHi promotes the paraxial mesoderm fate from NMP-like cells differentiating in vitro, whereas lower pHi favours the neural fate.

Reducing glycolytic activity by treating iPS cells differentiating in vitro with 2DG decreases the pHi of cells and increases *SOX1* expression (Fig. 2f, h). This effect can be significantly rescued by incubating cells cultured in 2DG-containing medium at a higher pH (Fig. 2h). In these conditions, *SOX1* expression decreased, and *AXIN2* expression increased (Fig. 2h). A similar rescue was observed in glucose-free medium (Fig. 2i). Thus, our in vivo and in vitro data suggest that pHi controls WNT signalling downstream of glycolysis in NMP-like cells.

The dynamic regulation of WNT signalling in differentiating iPS cells is somewhat unexpected as it occurs despite the constant presence of the WNT activator Chir in the culture medium. Chir inhibits glycogen synthase kinase 3β, which phosphorylates β-catenin and targets it for degradation[20,26]. In whole extracts from cultures of human iPS-derived PSM cells, we observed a stable expression of β-catenin and its non-phosphorylated (active) form between day 1 and day 4 (Fig. 3a). The downregulation of nuclear β-catenin and WNT targets

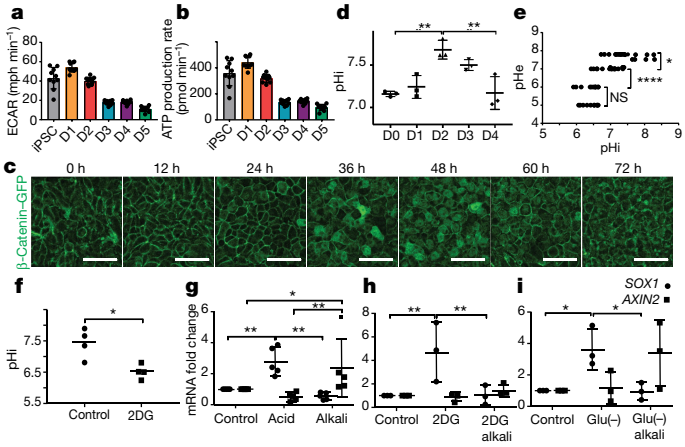

Fig. 2 | pHi and glycolysis decrease during in vitro differentiation of human iPS-derived PSM cells. a, **b**, Extracellular acidification rate (ECAR) (**a**) and glycolytic ATP production rate (**b**) in iPS cells (iPSCs) and day (D) 1–5 differentiated iPS cells. $n = 10$ replicates in 3 independent experiments. **c**, Snapshots from time-lapse imaging of eGFP-tagged β-catenin in differentiating iPS cells ($n = 3$ independent experiments). Scale bars, 50 µm. **d**, pHi analysis in human iPS cells differentiated to the PSM fate in vitro ($n = 3$). One-way ANOVA followed by Tukey's multiple comparisons test. $^{**}P < 0.01$. **e**, Analysis of the pHi using BCECF dye in D1–D2 human iPS cells differentiated to the PSM fate in vitro and cultured for 3 h in CL medium at different pH ($n = 6$ independent experiments). One-way ANOVA with Tukey's multiple comparisons test. $^{*}P = 0.023$, $^{****}P = 7.26 \times 10^{-6}$ and NS, $P = 0.999$. **f**, pHi analysis in human iPS cells cultured for 1 day in CL medium followed by 24 h in CL medium with 2DG ($n = 4$ for each condition). Unpaired, two-tailed *t*-test, control versus 5 mM 2DG: $^{*}P = 0.01$. **g**, *SOX1* and *AXIN2* expression in D2 human PSM-like cells cultured for 3 h in CL medium at different pH (*AXIN2* (control, acid and alkali): $n = 5$, *SOX1* (control and acid): $n = 5$ and *SOX1* (alkali): $n = 6$). Two-way ANOVA followed by Tukey's multiple comparisons test. $^{*}P < 0.05$ and $^{**}P < 0.01$. **h**, **i**, *SOX1* and *AXIN2* expression in human iPS cells cultured for 1 day in CL medium followed by a 24-h 2DG treatment (**h**) or in glucose-free (Glu(–)) CL medium (**i**) at normal or alkaline pH ($n = 3$ experiments for each condition). Two-way ANOVA followed by Tukey's multiple comparisons test. $^{*}P < 0.05$ and $^{**}P < 0.01$ (control: pH 7.0–7.2, acid: pH 6.3–6.5 and alkali: pH 7.5–7.8). In **a**, **b**, **d** and **g**–**i**, the mean ± s.d. is shown. In **f**, the bar indicates the mean. Exact *P* values can be found in the corresponding Source Data files.

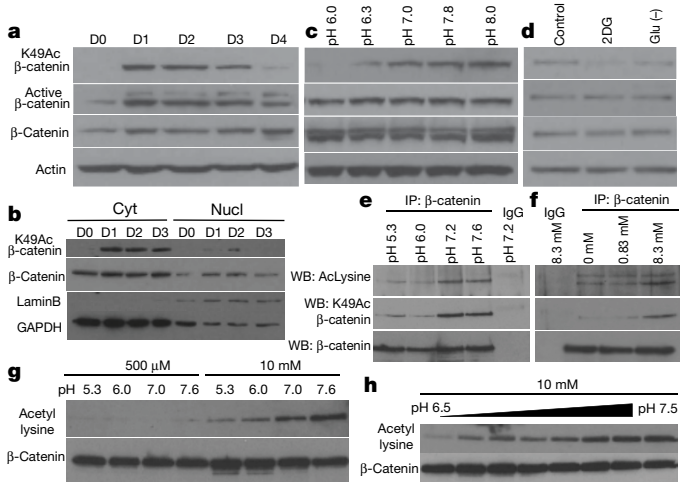

Fig. 3 | Regulation of β-catenin acetylation by glycolysis and pHi. a, Western blot analysis of whole-cell extracts prepared from human iPS cells differentiated to the PSM in vitro in CL medium, using anti-acetylated K49 (K49Ac) β-catenin, anti-active β-catenin, anti-actin and anti-β-catenin ($n = 3$). **b**, Western blot analysis of cytoplasmic (Cyt) and nuclear (Nucl) extracts prepared from human iPS cells differentiated to the PSM in vitro in CL medium, using anti-K49Ac β-catenin, anti-lamin B, anti-GAPDH and anti-β-catenin ($n = 3$). **c**, Western blot analysis of whole-cell extracts of D2 human iPS cells differentiated to the PSM in vitro in CL medium and cultured at different pH for 3 h, using anti-K49Ac β-catenin, anti-active β-catenin, anti-actin and anti-β-catenin ($n = 4$). **d**, Western blot analysis of whole-cell extracts of D2 human iPS cells differentiated to the PSM in CL medium in vitro and cultured for 6 h in 2DG and Glu(–) CL medium, using anti-K49Ac β-catenin, anti-active β-catenin, anti-actin and anti-β-catenin ($n = 3$). **e**, Immunoprecipitations (IP) of extracts of 2-day-old chicken embryos cultured at different pH with anti-β-catenin ($n = 3$). Western blot (WB) analysis was done using anti-acetylated lysine (AcLysine), anti-K49Ac β-catenin and anti-β-catenin. IgG was used as the control immunoprecipitation. **f**, Immunoprecipitations of extracts of 2-day-old chicken embryos cultured at different glucose concentrations with anti-β-catenin ($n = 4$). Western blot analysis was done using anti-AcLysine, anti-K49Ac β-catenin and anti-β-catenin. IgG was used as the control immunoprecipitation. **g**, Western blot analysis using anti-acetylated lysine (top) and anti-β-catenin (bottom). Recombinant β-catenin protein was incubated with 500 µM or 10 mM acetyl-CoA sodium salt in PBS at different pH conditions for 3 h at 37 °C ($n = 3$). **h**, Western blot analysis using anti-acetylated lysine (top) and anti-β-catenin (bottom). Recombinant β-catenin protein was incubated with 10 mM acetyl-CoA sodium salt in PBS at pH 6.5–7.5 for 3 h at 37 °C $n = 3$. For gel source data, see Supplementary Fig. 1.

observed despite Chir treatment suggests that events downstream of β-catenin stabilization are dynamically regulated in PSM cells. One such candidate is K49 β-catenin acetylation, which acts as a switch to control mesodermal versus neural gene activation in mouse embryonic stem cells[7]. We observed a dynamic expression of K49 acetyl β-catenin peaking at days 1–3 in vitro (Fig. 3a), which coincided with the peak of nuclear β-catenin (Fig. 3b). Switching differentiating iPS cells to acidic conditions for 3 h at day 2 led to a decrease in the levels of K49 acetylated β-catenin, whereas exposure to alkaline conditions increased acetylated β-catenin levels (Fig. 3c). In human PSM cells, K49 acetylated β-catenin expression decreased in the absence of glucose (Fig. 3d). In all of these conditions, the levels of non-phosphorylated and total β-catenin remained stable (Fig. 3c, d). Stimulating global acetylation by treating differentiating cells with sodium acetate led to an increase in K49 β-catenin acetylation, whereas β-catenin and its non-phosphorylated form remained stable (Extended Data Fig. 5a). Acetate treatment resulted in upregulation of *MSGN1* and decrease of *SOX1* expression (Extended Data Fig. 5b). Thus, our data suggest that K49 β-catenin acetylation has a role in the regulation of WNT signalling during PSM differentiation in vitro.

β-catenin is also acetylated in the PSM of chicken embryos (Fig. 3e). Exposure of 2-day-old chicken embryos to low pH (pH 5.3 or 6.0), but not to high pH (pH 7.6), decreased acetylated β-catenin levels in the PSM (Fig. 3e). By contrast, the levels of active non-phosphorylated and of total β-catenin were stable when embryos were exposed to buffers of different pH (Fig. 3e, Extended Data Fig. 6a). Thus, β-catenin acetylation is affected by pH changes as observed in vitro. Reduction of acetylated and K49 acetyl, but not total or non-phosphorylated, β-catenin levels was also observed when reducing glucose concentration or treatment with CNCn in embryos cultured in minimal medium (Fig. 3f, Extended Data Figs. 3f, 6b). Conversely, treatment of 2-day-old chicken embryos with sodium acetate led to an upregulation of K49 β-catenin acetylation (Extended Data Fig. 5c). This also resulted in a significant upregulation of *AXIN2* and *MSGN1* (Extended Data Fig. 5d, e). Together, these data show that β-catenin acetylation levels in the chicken embryo PSM can be modulated by pHi, glucose or acetate independently of total and non-phosphorylated β-catenin levels.

The pHi can control the protonation of specific histidines in proteins that act as pH sensors, leading to changes in the protein properties[8,27]. While acetylation of protein substrates such as histones is largely regulated by histone acetyltransferases and histone deacetylases, non-enzymatic acetylation of proteins has also been demonstrated in

many different cell types[28]. This chemical addition of acetyl residues to cellular proteins can be regulated by the pHi of cells[29]. Thus, the high pHi observed in PSM cells downstream of glycolysis might provide favourable chemical conditions for non-enzymatic β-catenin acetylation. To test this possibility, we incubated recombinant β-catenin protein with acetyl-CoA sodium salt in vitro at pH 5.0, pH 6.3, pH 7.2 and pH 7.6 for 3 h at 37 °C. A clear dose-dependent increase of β-catenin acetylation was detected when the pH was raised (Fig. 3g). Even small pH increments within a physiological range (pH 6.5–7.5) led to a dose-dependent increase of β-catenin acetylation (Fig. 3h, Extended Data Fig. 6c).

Decreasing the pHi in tumour cells was proposed as a therapeutic strategy to treat cancer as it leads to growth arrest, largely owing to inhibition of mechanistic target of rapamycin[6,12]. In WNT-addicted tumour cells, lowering the pHi was recently shown to inhibit WNT signalling[30], as reported here for differentiating tail bud cells. Thus, our findings further emphasize the tight similarity between the developing tail bud cells and cancer cells that exhibit high Warburg metabolism, resulting in high pHi and low pHe[6].

Online content

Any methods, additional references, Nature Research reporting summaries, source data, extended data, supplementary information, acknowledgements, peer review information; details of author contributions and competing interests; and statements of data and code availability are available at https://doi.org/10.1038/s41586-020-2428-0.

1. Bénazéraf, B. et al. A random cell motility gradient downstream of FGF controls elongation of an amniote embryo. *Nature* **466**, 248–252 (2010).
2. Vander Heiden, M. G., Cantley, L. C. & Thompson, C. B. Understanding the Warburg effect: the metabolic requirements of cell proliferation. *Science* **324**, 1029–1033 (2009).
3. Oginuma, M. et al. A gradient of glycolytic activity coordinates FGF and Wnt signaling during elongation of the body axis in amniote embryos. *Dev. Cell* **40**, 342–353.e10 (2017).
4. Henrique, D., Abranches, E., Verrier, L. & Storey, K. G. Neuromesodermal progenitors and the making of the spinal cord. *Development* **142**, 2864–2875 (2015).
5. Kimelman, D. Tales of tails (and trunks): forming the posterior body in vertebrate embryos. *Curr. Top. Dev. Biol.* **116**, 517–536 (2016).
6. Parks, S. K., Chiche, J. & Pouysségur, J. Disrupting proton dynamics and energy metabolism for cancer therapy. *Nat. Rev. Cancer* **13**, 611–623 (2013).
7. Hoffmeyer, K., Junghans, D., Kanzler, B. & Kemler, R. Trimethylation and acetylation of β-catenin at lysine 49 represent key elements in ESC pluripotency. *Cell Rep.* **18**, 2815–2824 (2017).
8. Webb, B. A., Chimenti, M., Jacobson, M. P. & Barber, D. L. Dysregulated pH: a perfect storm for cancer progression. *Nat. Rev. Cancer* **11**, 671–677 (2011).
9. Miesenböck, G., De Angelis, D. A. & Rothman, J. E. Visualizing secretion and synaptic transmission with pH-sensitive green fluorescent proteins. *Nature* **394**, 192–195 (1998).
10. Grillo-Hill, B. K., Webb, B. A. & Barber, D. L. Ratiometric imaging of pH probes. *Methods Cell Biol.* **123**, 429–448 (2014).
11. Hamburger, V. & Hamilton, H. L. A series of normal stages in the development of the chick embryo. 1951. *Dev. Dyn.* **195**, 231–272 (1992).
12. Balgi, A. D. et al. Regulation of mTORC1 signaling by pH. *PLoS ONE* **6**, e21549 (2011).
13. Chiche, J. et al. In vivo pH in metabolic-defective Ras-transformed fibroblast tumors: key role of the monocarboxylate transporter, MCT4, for inducing an alkaline intracellular pH. *Int. J. Cancer* **130**, 1511–1520 (2012).
14. Fellenz, M. P. & Gerweck, L. E. Influence of extracellular pH on intracellular pH and cell energy status: relationship to hyperthermic sensitivity. *Radiat. Res.* **116**, 305–312 (1988).
15. Chambard, J. C. & Pouyssegur, J. Intracellular pH controls growth factor-induced ribosomal protein S6 phosphorylation and protein synthesis in the G0→G1 transition of fibroblasts. *Exp. Cell Res.* **164**, 282–294 (1986).
16. Yoon, J. K. & Wold, B. The bHLH regulator pMesogenin1 is required for maturation and segmentation of paraxial mesoderm. *Genes Dev.* **14**, 3204–3214 (2000).
17. Chal, J. et al. Differentiation of pluripotent stem cells to muscle fiber to model Duchenne muscular dystrophy. *Nat. Biotechnol.* **33**, 962–969 (2015).
18. Chal, J. et al. Generation of human muscle fibers and satellite-like cells from human pluripotent stem cells in vitro. *Nat. Protoc.* **11**, 1833–1850 (2016).
19. Diaz-Cuadros, M. et al. In vitro characterization of the human segmentation clock. *Nature* **580**, 113–118 (2020).
20. Nusse, R. & Clevers, H. Wnt/β-catenin signaling, disease, and emerging therapeutic modalities. *Cell* **169**, 985–999 (2017).
21. Chalamalasetty, R. B. et al. Mesogenin 1 is a master regulator of paraxial presomitic mesoderm differentiation. *Development* **141**, 4285–4297 (2014).
22. Aulehla, A. et al. Wnt3a plays a major role in the segmentation clock controlling somitogenesis. *Dev. Cell* **4**, 395–406 (2003).
23. Nowotschin, S., Ferrer-Vaquer, A., Concepcion, D., Papaioannou, V. E. & Hadjantonakis, A. K. Interaction of Wnt3a, Msgn1 and Tbx6 in neural versus paraxial mesoderm lineage commitment and paraxial mesoderm differentiation in the mouse embryo. *Dev. Biol.* **367**, 1–14 (2012).
24. Aulehla, A. et al. A β-catenin gradient links the clock and wavefront systems in mouse embryo segmentation. *Nat. Cell Biol.* **10**, 186–193 (2008).
25. Yamaguchi, T. P., Takada, S., Yoshikawa, Y., Wu, N. & McMahon, A. P. *T* (Brachyury) is a direct target of Wnt3a during paraxial mesoderm specification. *Genes Dev.* **13**, 3185–3190 (1999).
26. Wagman, A. S., Johnson, K. W. & Bussiere, D. E. Discovery and development of GSK3 inhibitors for the treatment of type 2 diabetes. *Curr. Pharm. Des.* **10**, 1105–1137 (2004).
27. White, K. A. et al. β-Catenin is a pH sensor with decreased stability at higher intracellular pH. *J. Cell Biol.* **217**, 3965–3976 (2018).
28. Wagner, G. R. & Hirschey, M. D. Nonenzymatic protein acylation as a carbon stress regulated by sirtuin deacylases. *Mol. Cell* **54**, 5–16 (2014).
29. Paik, W. K., Pearson, D., Lee, H. W. & Kim, S. Nonenzymatic acetylation of histones with acetyl-CoA. *Biochim. Biophys. Acta* **213**, 513–522 (1970).
30. Melnik, S. et al. Cancer cell specific inhibition of Wnt/β-catenin signaling by forced intracellular acidification. *Cell Discov.* **4**, 37 (2018).

Methods

Chicken embryo culture

All animal experiments were performed in accordance with all relevant guidelines and regulations. The Office for Protection from Research Risks has interpreted 'live vertebrate animal' to apply to avians (for example, chick embryos) only after hatching. All of the studies proposed in this project only concern early developmental stages (before 5 days of incubation); therefore, no Institutional Animal Care and Use Committee-approved protocol is required. Fertilized chicken eggs were obtained from commercial sources. Eggs were incubated at 38 °C in a humidified incubator, and embryos were staged according to HH[11]. We cultured chicken embryos mainly from stage 9HH at 37 °C on a ring of Whatman paper on agar plates as described in the Easy Culture (EC) protocol[31]. Chemically defined plates (3.5-mm petri dish X25) were produced by combining an agarose solution (0.15 g agarose melted by heating in 25 ml ddH_2O (MilliQ)) and 25 ml 2× DPBS solution with 8.3 mM, 0.83 mM and 0 mM glucose. For chemically defined medium, a 2× PBS solution (pH 5.3, pH 6.0, pH 7.2 and pH7.6) was prepared by combining 50 ml 10× DPBS (D1283, Sigma) and 450 ml of ddH_2O, adding (0 g: pH 5.3, 0.15g: pH 6.0, 0.6 g: pH 7.2 and 1.5 g: pH 7.6) sodium bicarbonate (S5761, Sigma) and 2.5 ml penicillin–streptomycin solution (Gibco (10,000 U/ml)). Embryos were prepared on a ring paper as for EC culture and incubated on the agarose plates in 2 ml of chemically defined medium. For drug treatments, 2 mM 2DG (Sigma), 5 mM CNCn (Sigma) and 10 mM sodium acetate (Sigma) were mixed to a chemically defined plate (8.3 mM glucose PBS plate, pH 7.2).

Time-lapse microscopy and axis elongation measurements

Stage 9HH chicken embryos were cultured ventral side up on a microscope stage using a custom-built time-lapse station[1]. We used a computer controlled, wide-field (×10 objective) epifluorescent microscope (Leica DMR) workstation, equipped with a motorized stage and cooled digital camera (QImaging Retiga 1300i), to acquire 12-bit greyscale intensity images (492 × 652 pixels). For each embryo, several images corresponding to different focal planes and different fields were captured at each single time-point (frame). The acquisition rate used was 10 frames per hour (6 min between frames). To quantify axis elongation length, the last formed somite at the beginning of the time-lapse experiment was taken as a reference point, and the position of the Hensen's node with respect to this somite was tracked as a function of time using the manual tracking plug-in in ImageJ[32].

Whole-mount in situ hybridization

Stage 9HH embryos were cultured at 38 °C in chemically defined medium. After 10 h of incubation, embryos were fixed in 4% paraformaldehyde. Whole-mount in situ hybridization was carried out as previously described[33]. Probes for *AXIN2*[34], *CMESPO* (also known as *Mesogenin1*)[35], *SOX2* and *SAX1*[36] have been described. Probes for *MCT1* were generated from chicken embryo cDNA by PCR using published sequences.

Plasmid preparation and electroporation for chicken embryo

The ratiometric pH sensor pHluorin[9] was used to generate the expression vector pCAGG-pHluorin-IRES2-Td-Tomato. The full-length pHluorin sequence was subcloned in the pENTR-1A vector (Invitrogen) and inserted into a pCAGGS-IRES2-tdt-RFA destination vector using the Gateway system (Invitrogen). Chicken embryos ranging from stage 6HH to stage 7HH were prepared for EC culture. A DNA solution (1.0–5.0 μg/μl) was microinjected in the space between the vitelline membrane and the epiblast at the anterior primitive streak level, which contains the precursors of the paraxial mesoderm. In vitro electroporations were carried out with five successive square pulses of 8 V for 50 ms, keeping a 4-mm distance between the anode and the cathode using Petri dish-type electrodes (CUY701P2, Nepa Gene) and a CUY21 electroporator (Nepa Gene).

pHi measurement for chicken embryo

To measure the pHi in PSM and tail bud cells, stage 4–5HH chicken embryos were electroporated with the pCAGGS-pHluorin-IRES2-Td-Tomato construct, which contains the ratiometric pH biosensor pHluorin[9], and cultured until stage 12HH at 38 °C. Embryos strongly expressing the constructs were subsequently selected based on tdTomato expression in the PSM and tail bud. We first tested whether pHluorin can accurately report on pHi differences when electroporated in the chicken embryo. Embryos were electroporated at the anterior primitive streak level with the pHluorin construct to target tail bud and PSM cells as described previously[37], and they were reincubated until they reached stage 12HH. Embryos were then incubated in different buffers (pH 5.5, pH 6.5 and pH 7.5) from the pH calibration buffer kit (Molecular probes) with 10 μM of the protonophores nigericin and valinomycin at 37 °C for 30 min. Exposure to the protonophores allows the cells' pHi to equilibrate to the buffer pH. Then embryos were mounted on MatTek glass-bottom dishes soaked in pH calibration buffer (pH 5.5, pH 6.5 and pH 7.5). Images were captured using a laser scanning confocal microscope (TCS SP5, Leica or LSM780, Zeiss) at 37 °C in humidified atmosphere. The protonophore treatment completely abolished the gradient of the pHluorin 488/405 signal ratio and the average emission signal ratio under 488/405-nm excitation decreased as pH increased (Extended Data Fig. 1), indicating that the pHluorin reporter electroporated in vivo can report on pHi changes. However, because it is impossible to perform the different steps required for calibration in the same embryo, different electroporated embryos were used for each pH value and for experimental measurements. As a result, the absolute value of the pH could not be defined and only relative pH differences are discussed. Thus, for all in vivo measurements, we only compared the 405-to-488-nm fluorescence ratios.

To measure the pHi in vivo, embryos were electroporated at stage 4–5HH with the pHluorin construct and cultured in EC culture until stage 9HH, and then cultured for 10 h with and without 2DG in EC cultures or in chemically defined conditions before mounting. Next, embryos were mounted on MatTek glass-bottom slides on a thin albumin/agar gel in the same culture conditions. Images were captured as described above. After image capture, three-channel *z*-stacks (.lif) of individual embryos were exported using Fiji into single-channel single-plane images (.png) for import into GoFig. 2 software (www.gofigure2.org)[38]. Spherical segmentations of 9-μm radius were generated manually on the tdTomato channel image to encircle single cells on the raw images. Intensities of the 405-nm-excited and 488-nm-excited pHluorin signals were automatically calculated within the segmentations by GoFig. 2. The measurements were exported for further analysis in custom-made MATLAB routines (MathWorks). To compare pH between different embryos, segmentations from individual embryos measured in the same-day experiment were averaged to obtain a global ratio, followed by unpaired *t*-tests. To compare pH between different regions of individual embryos, segmentations were first normalized to the global ratio to minimize the contribution of embryo-to-embryo variation of overall signal intensity, followed by paired *t*-tests. In Fig. 1b, average values are calculated every 30 segmented cells along the anterior–posterior axis. The normalized average 488/405-nm ratio in the anterior and posterior PSM in control and experimental embryos were calculated from the average of 40 posterior-most and 40 anterior-most cells. Black lines connect the anterior and posterior ends of the same embryo in Fig. 1d, g. To calculate the average 488/405-nm fluorescence ratio of 2-day-old chicken embryos shown in Fig. 1f, h, in each sample, the average ratio (black dot) was obtained by averaging all cells (n = 50–250 per embryo). Samples were then pooled to compare the average ratio. The ratio of fluorescence intensity is shown with Fire colour using ImageJ.

Alternatively, BCECF-AM (B1150, Thermo Fisher Scientific) was used to analyse the pHi in PSM explants. PSM explants were dissected in PBS with Ca^{2+} and Mg^{2+} (Sigma) using collagenase type IV to loosen embryonic tissue. After dissection, explants were incubated for 1 h with 20 μM BCECF diluted in culture medium (DMEM/F12, 10% FBS and 1% penicillin–streptomycin) at 37 °C and 5% CO_2. Then, explants were washed with PBS with Ca^{2+} and Mg^{2+}. BCECF fluorescence was measured with a confocal microscope (LSM780, Zeiss) at two excitation wavelengths (405 nm and 488 nm), both collected at a collection window of 515–555 nm. Statistical significance was assessed by two-sided, paired *t*-test.

Maintenance and differentiation of human iPS cells

Human stem cell work was approved by Partners Human Research Committee (protocol number 2017P000438/PHS). We complied with all relevant ethical regulations. Written informed consent from the donors of the iPS cells was obtained at the time of sample collection. The cell line NCRM1 (RUCDR, Rutgers University) was used for most human iPS cell experiments. For Fig. 3b, the previously described MSGN1-RepV reporter line was used[39]. We also obtained the monoallelic mEGFP-tagged *CTNNB1* WTC iPS cell line from the Allen Cell Collection at the Coriell Institute (cat. no. AICS-0058-067). Authentication was unnecessary owing to the unique morphology of human iPS cells, as well as their unique differentiation potential. All cell lines tested negative for mycoplasma contamination. Human iPS cells were cultured on Matrigel (BD Biosciences)-coated dishes in mTeSR medium (STEMCELL Technologies). Differentiation was performed as previously described[18]. In brief, cells were plated at a density of 30,000–35,000 cells per cm^2 in mTeSR supplemented with 10 μM Y-27362 dihydrochloride (Rocki; 1254, Tocris Bioscience). The next day (day 0 of differentiation), the medium was changed to DMEM/F12 GlutaMAX (10565-018, Gibco) supplemented with insulin–transferrin–selenium (ITS, Gibco), 3 μM Chir99021 (4423, Tocris) and 0.5 μM LDN193189 (04-0074, Stemgent) (CL medium). At differentiation day 3, 20 ng/ml FGF (450-33, PeproTech) was added for an additional 3 days.

Culture medium preparation

To examine the effect of medium pH, cells were incubated in medium buffered at different pH for 3 h at differentiation day 2. To adjust the medium pH, HCl and sodium bicarbonate (S5761, Sigma) were used and the pH of the medium was measured using a pH meter (Mettler Toledo) or pH indicator papers (pH 6.0–8.1) (2629-990, GE Healthcare Life Sciences). Before the experiments, the medium pH was equilibrated by incubation in 5% CO_2 at 37 °C for 24 h.

To examine the effect of the glucose-free condition, cells were incubated in glucose(−) medium for 6 h at differentiation day 2 or for 24 h at differentiation day 1. 2DG (5 mM; D8375, Sigma) was used in 5 mM D-(+)-glucose (G7021, Sigma) containing DMEM medium (D9807-02, United States Biologicals) to inhibit glycolysis. Culture in CL medium with 2 or 10 mM sodium acetate (S2889, Sigma) for 24 h at differentiation day 1 was used to increase the acetylation level.

Quantitative RT–PCR

RNA was extracted using TRIzol (15596-018, Invitrogen), followed by precipitation with chloroform (288306, Sigma) and ethanol (459836, Sigma). RT–PCR was performed using 1 μg total RNA using SuperScriptIII Reverse Transcriptase (18080-051, Invitrogen). qPCR assays were run on a Bio-Rad CFX384 thermocycler using the iTaq Universal SYBR Green kit (cat. no. 1725124, Bio-Rad). β-Actin was used as an internal control.

The following primers were used for PCR of human genes. *ACTIN* (forward: ccaaccgcgagaagatga; reverse: ccagaggcgtacagggatag), *MSGN1* (forward: ctgggactggaaggacagg; reverse: acagctggacagggagaaga), *TBX6* (forward: aagtaccaaccccgcataca; reverse: taggctgtcacggagatgaa), *AXIN2* (forward: ggagtgcgttcatggtttct; reverse: tgcatgtgtcaatggtaggg) and *SOX1* (forward: ggaatgggaggacaggattt; reverse: acttttatttctcggcccgt).

The following primers were used for PCR of chicken genes. *BETA-ACTIN* (Gg_ACTB_1_SG QuantiTect Primer Assay), *AXIN2* (Gg_AXIN2_1_SG QuantiTect Primer Assay), *T* (forward: cgaggagatcacagctttaaaaatt; reverse: tcatttctttcctttgcgtcaa), *MSGN1* (forward: aaagccagtgagagggagaa; reverse: ggtgcacttgagggtctgta), *SOX2* (forward: gcagagaaaaggg aaaaagga; reverse: tttcctagggaggggtatgaa) and *SAX1* (forward: cagctttcacctacgagcag; reverse: tggaaccagatcttcacctg).

Measurement of pHi in human iPS cells

The BCECF-AM pH sensitive dye (B1150, Thermo Fisher Scientific) was used to analyse the pHi in human iPS cells according to the manufacturer's instructions. Human iPS cells were differentiated to day 1 in a 96-well plate format, then incubated for 3 h in differentiation media calibrated at different pH values (described in 'Maintenance and differentiation of human iPS cells' and 'Culture medium preparation'). After 3 h of incubation, cells were washed with HBSS (14025-092, Gibco), to eliminate any exogenous source of nonspecific esterases that could prematurely cleave the lipophilic-blocking groups of the BCECF-AM interfering with permeabilization of the dye, cells were then incubated in 1 μM BCECF-AM ester solution (diluted in HBSS) for 20 min at 37 °C. Next, cells were washed in HBSS, to remove non-incorporated BCECF-AM ester that remained in the media, and incubated at 37 °C for 10 min in fresh differentiation medium calibrated at their corresponding pH values (matching the pH of the initial 3 h incubation step). To measure fluorescence of the dye, we replaced the medium with calibration buffers (P35379, Thermo Fisher Scientific; adjusted by HCl or NaOH if necessary) to the corresponding pH values of the differentiation medium (matching the pH of the initial 3-h incubation step), and immediately (less than 5 min after the last medium change; replacing differentiation medium by calibration buffer) measured the ratio of emission intensity at 535 nm, by exciting the dye at 490 nm and at its isosbestic point of 440 nm using a GloMax-Multi Detection System (Promega). To determine the absolute pH values, we generated a calibration curve by incubating, in parallel, cells in wells with calibration buffer at five different pH values (P35379, Thermo Fisher Scientific; 4.5–8.5, the last value adjusted by NaOH) with the addition of the protonophores nigericin and valinomycin (each at 10 μM) at 37 °C for 15 min after BCECF-AM ester incubation. As can be seen on the calibration curve shown in Extended Data Fig. 7, significant variation is observed for individual pH measurements, thus precluding conclusions on exact pH values. Fluorescent acquisition for calibration wells was done as described above.

Lactate assay

To detect lactate production by the differentiated iPS cells, we used a lactate assay kit (K607-100, Bio Vision) according to the manufacturer's instructions. Measurement of optical density at 560 nm was performed using the GloMax-Multi Detection System (Promega). Values were normalized by total protein amount in each well. Lactate detection in the chicken tail bud was carried out as previously described[3].

ECAR and glycolytic ATP production measurement

NCRM1 iPS cells were differentiated on consecutive days to obtain day 1–5 populations on the day of the seahorse assay. iPS cells and day 1–5 differentiated cells were dissociated using TryplE Express (cat. no. 12605036, Gibco) and reseeded onto Matrigel-coated Seahorse XF96 Cell Culture Microplates (cat. no. 101085-004, Agilent) at a density of 50,000 cells per well in Seahorse XF DMEM assay medium (cat. no. 103575-100, Agilent). After allowing cells to attach for 2 h, the assay medium was refreshed and the Seahorse XF Real-Time ATP Rate Assay (cat. no. 103592-100, Agilent) was carried out according to the manufacturer's instructions. All samples were run in ten replicates in a Seahorse XFe96 Analyzer and the data were analysed in Wave and Microsoft Excel using macros provided by the manufacturer.

Immunocytochemistry

Cells were washed with PBS and fixed in 4% paraformaldehyde/PBS for 20 min at room temperature. Fixed cells were washed with PBS, then blocked and permeabilized with 3% FBS and 0.1% Triton X-100/PBS at room temperature for 30 min. Cells were then incubated with anti-β-catenin (1:500; 610153, BD) and a chicken anti-GFP (1:800; ab13970, Invitrogen) diluted in PBS containing 3% FBS and 0.1% Triton X-100/PBS at 4 °C overnight, and next with secondary antibodies conjugated with Alexa 488 and Alexa 594 (1:500; A11039 and A11037, respectively, Invitrogen) for 30 min at room temperature. Images were captured using a laser scanning confocal microscope (LSM780, Zeiss).

Quantification of β-catenin nuclear localization

Nuclear localization of β-catenin was measured in cultures immunostained with the anti-β-catenin using the Fiji software. First, we split the channels and smoothened the Hoechst staining images using the 'Gaussian Blur' filter. Then, we binarized the image, cut the border of adjacent cells using 'watershed' and eliminated the β-catenin expression in the outermost of the nucleus area using the 'erode' filter. Next, we manually drew the contours of the nucleus and used the 'analyze particles' tool to measure the signal intensity of β-catenin in each nucleus.

Time-lapse imaging of β-catenin–GFP fusion the iPS cell line

iPS cells containing a β-catenin–GFP fusion were differentiated as described above in 24-well glass-bottom plates and imaged on a Zeiss LSM 780 point-scanning confocal inverted microscope fitted with a large temperature incubation chamber and a CO_2 module. An argon laser at 488 nm and 2% power was used to excite eGFP through a ×20 Plan Apo (NA 0.8) objective. Images were acquired every hour from the onset of differentiation until day 3 (72 h). Representative images corresponding to 0, 12, 24, 36, 48, 60 and 72 h were selected for illustration. Images were subjected to background subtraction and gaussian blurring in ImageJ for improved quality.

Western blotting

Cells were collected with lysis buffer (50 mM Tris-HCl pH 8.0, 100 mM NaCl, 5 mM $MgCl_2$, 0.5% Triton X-100, proteinase inhibitor cocktail (78443S, Promega) and 250 U/ml Benzonase (Sigma-Aldrich)) and incubated on ice for 30 min. After addition of SDS (1% final), protein concentrations were measured using a protein assay kit (Bio-Rad). The protein solution (10–20 µg) was boiled in sample buffer and then ran on 10% or 12.5% SDS–PAGE. After transfer from the gel to a polyvinylidene fluoride membrane (Millipore), the membrane was immersed in buffer containing 5% skimmed milk at room temperature for 1 h. Membranes were then incubated with the primary antibody (diluted in 5% skimmed milk) overnight at 4 °C. The next day, membranes were washed with PBT (PBS and 0.1% Tween 20) and incubated with goat anti-rabbit IgG secondary antibody and horseradish peroxidase conjugate (1:1,000–1:10,000; 31460, Invitrogen), or goat anti-mouse IgG secondary antibody and horseradish peroxidase conjugate (1:1,000–1:10,000; 31430, Invitrogen) for 1 h at room temperature. Immunoreactive bands were visualized with ECL Blotting Reagents (RPN2109, GE Healthcare) or SuperSignal West Pico PLUS Chemiluminescent Substrate (34577, Thermo Scientific) and detected using a Kodak X-OMAT 200A processor. After detecting the bands, membranes were washed with PBT and incubated in stripping buffer (2% SDS, 62.5 mM Tris-HCl pH 6.8 and 0.7% 2-mercaptoethanol) for 30 min at 50 °C to remove the antibody. Subsequent stainings were performed after removing the antibody. We used an anti-acetyl-β-catenin (Lys49) (1:1,000; 9534S, Cell Signaling Technology), anti-active-β-catenin (1:1,000; 05-665, Millipore), anti-β-catenin (1:1,000; 610153, BD), anti-actin (1:5,000; MAB1501, Millipore), anti-lamin B1 (1:5,000; ab16048, abcam) and anti-GAPDH (1:1,000; ab125247, abcam).

For chicken experiments, stage 9HH chicken embryos were incubated at 37 °C in different culture conditions (different pH or glucose concentrations) as described above. After 8 h of incubation, the posterior end of embryos was dissected and pooled (three embryos for each sample). Samples were prepared, and western blots were performed as for human iPS cell experiments.

Immunoprecipitation

Two-day-old chicken embryos were cultured on agar plates for 8 h as described above and lysed using the lysis buffer of the Immuno-precipitation kit (ab206996, abcam). Total protein concentration was adjusted to 100 µg per sample. Each sample was immunoprecipitated using 1 µg anti-β-catenin (610153, BD) or 1 µg normal mouse IgG (ab188776, abcam) overnight at 4 °C according to the manufacturer's instructions. After three washes using the kit's washing buffer, samples were diluted into 2× sampling buffer, then western blotting was performed as described above using anti-acetyl-β-catenin (Lys49) (1:1,000; 9534S, Cell Signaling Technology), anti-acetyl lysine (1:1,000; 9441, Cell Signaling) and anti-β-catenin (1:1,000; 610153, BD).

In vitro acetylation of β-catenin proteins

Recombinant human β-catenin protein (20 µg; ab63175, abcam) was incubated with 500 µM or 10 mM acetyl-CoA sodium salt (A2056, Sigma) in PBS solutions (final volume: 20 µl) at different pH conditions for 3 h at 37 °C. PBS solutions were prepared from 10× DPBS (D1283, Sigma), adding different amounts of sodium bicarbonate (S5761, Sigma). After incubation, 10 µl of each sample were run on a 10% SDS–PAGE gel. Western blot was performed as described above using anti-acetyl lysine (1:1,000; 9441, Cell Signaling Technology) and anti-β-catenin (1:1,000; 610153, BD).

Nuclear fraction

Nuclear and cytoplasmic extractions were performed using the NE-PER Nuclear and Cytoplasmic Extraction kit (78833, Thermo Fisher Scientific) in accordance with the manufacturer's instructions. After extraction, proteins were analysed by western blotting as described above.

Statistical analysis

Statistical analyses were performed with Prism 7.0 software (GraphPad). *P* values <0.05 were considered to be significant. The statistical methods used in the analysis are described in the figure legends.

Reporting summary

Further information on research design is available in the Nature Research Reporting Summary linked to this paper.

Data availability

All data generated or analysed during this study are included in this published article (and its Supplementary Information). Source data are provided with the paper.

Code availability

The custom MATLAB code used to process the 3D segmentations of pH measurements is available at https://github.com/amichaut/pHanalysis.

31. Chapman, S. C., Collignon, J., Schoenwolf, G. C. & Lumsden, A. Improved method for chick whole-embryo culture using a filter paper carrier. *Dev. Dyn.* **220**, 284–289 (2001).
32. Denans, N., Iimura, T. & Pourquié, O. Hox genes control vertebrate body elongation by collinear Wnt repression. *eLife* **4**, e04379 (2015).
33. Henrique, D. et al. Expression of a Delta homologue in prospective neurons in the chick. *Nature* **375**, 787–790 (1995).
34. Krol, A. J. et al. Evolutionary plasticity of segmentation clock networks. *Development* **138**, 2783–2792 (2011).

35. Buchberger, A., Bonneick, S. & Arnold, H. Expression of the novel basic-helix-loop-helix transcription factor cMespo in presomitic mesoderm of chicken embryos. *Mech. Dev.* **97**, 223–226 (2000).
36. Diez del Corral, R., Breitkreuz, D. N. & Storey, K. G. Onset of neuronal differentiation is regulated by paraxial mesoderm and requires attenuation of FGF signalling. *Development* **129**, 1681–1691 (2002).
37. Iimura, T. & Pourquié, O. Manipulation and electroporation of the avian segmental plate and somites in vitro. *Methods Cell Biol.* **87**, 257–270 (2008).
38. Xiong, F. et al. Specified neural progenitors sort to form sharp domains after noisy Shh signaling. *Cell* **153**, 550–561 (2013).
39. Chal, J. et al. Recapitulating early development of mouse musculoskeletal precursors of the paraxial mesoderm in vitro. *Development* **145**, dev157339 (2018).

Acknowledgements We thank N. Perrimon and members of the Pourquié laboratory for critical reading of the manuscript and discussions. Y.H. acknowledges Grant-in-Aid for JSPS Fellows (29-456). Research in the Pourquié laboratory was funded by a grant from the US National Institutes of Health (5R01HD085121). F.X. acknowledges the National Institutes of Health K99 award HD092582. This work was supported by AMED (JP19gm5010001 to T.I.), a Grant-in-Aid for Scientific Research on Innovative Areas (25117720 to T.I. and 19H04768 to M.O.), Scientific Research (B) (16H05141 and 19H03412 to T.I.) and Scientific Research (C) (19K06673 to M.O.).

Author contributions M.O. designed, performed and analysed the chicken embryo experiments and the in vitro acetylation study of purified β-catenin with help from O.A.T. Y.H. designed, performed and analysed the human iPS cell experiments with help from M.D.-C. and O.A.T. A.M. performed the in vivo BCECF pH measurements. F.X. performed the in vivo quantitative analysis of pHi. O.P. wrote the manuscript and supervised the project. All authors discussed and agreed on the results and commented on the manuscript.

Competing interests O.P. is a scientific founder of Anagenesis Biotechnologies. The other authors declare no competing interests.

Additional information

Supplementary information is available for this paper at https://doi.org/10.1038/s41586-020-2428-0.
Correspondence and requests for materials should be addressed to O.P.
Peer review information *Nature* thanks Matthew Hirschey, Jacques Pouyssegur and the other, anonymous, reviewer(s) for their contribution to the peer review of this work.
Reprints and permissions information is available at http://www.nature.com/reprints.

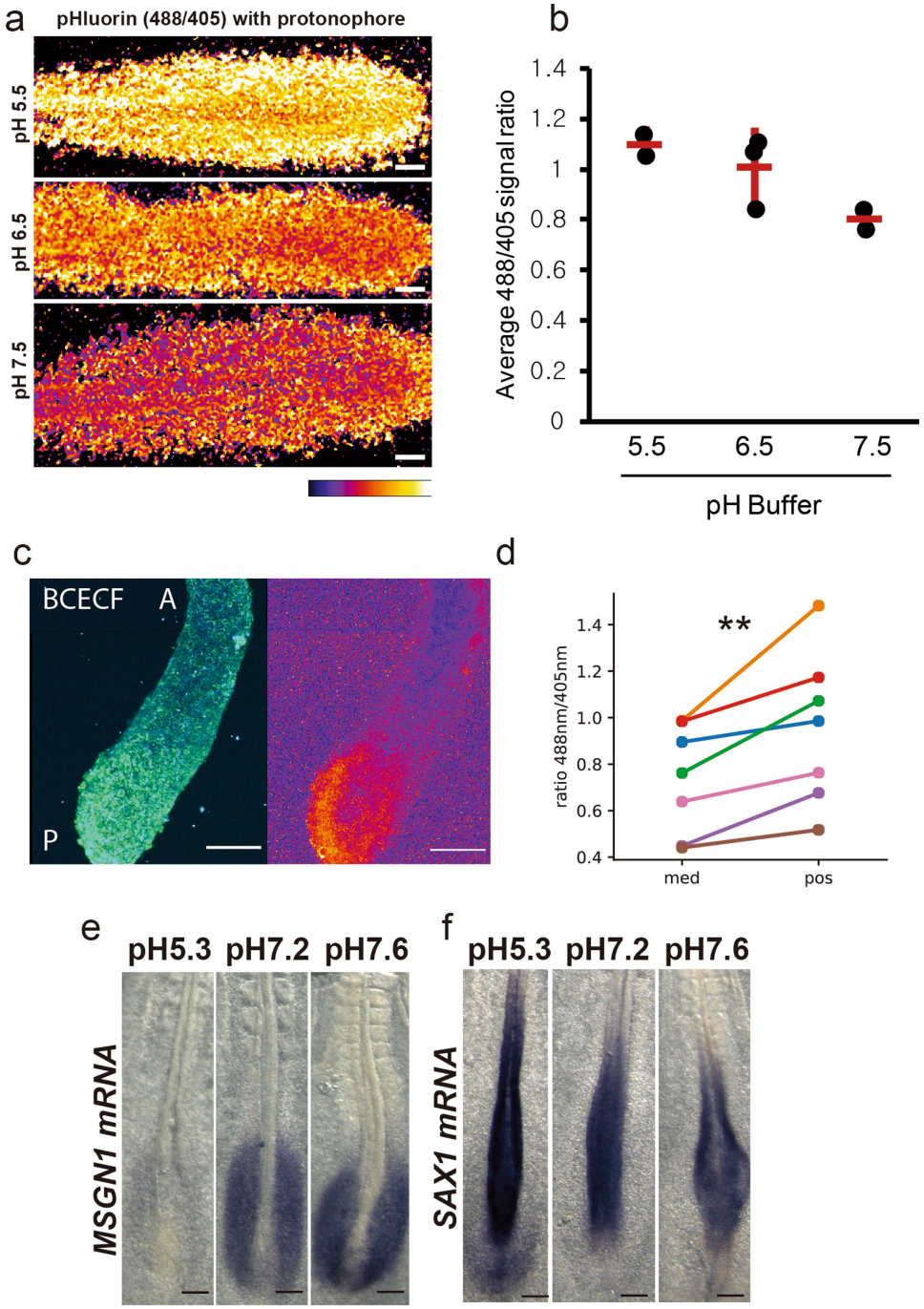

Extended Data Fig. 1 | Analysis of the pHi in the chicken embryo in vivo. **a**, Ratiometric live expression of pHluorin (488/405 nm) detected in the posterior domain of electroporated embryos exposed to different pH buffers and nigericin and valinomycin ($n = 7$). Fluorescence intensity is shown by a pseudocolour image (Fire colour) using ImageJ. The yellow signal indicates lower pH. The ventral view shows the anterior region to the left. Scale bars, 100 µm. **b**, Each dot represents the average 488/405-nm signal ratio of about 300 single cells segmented in one embryo ($n = 2$ for pH 5.5, $n = 3$ for pH 6.5 and $n = 2$ for pH 7.5). Embryos were treated for 20 min in different pH buffers with the protonophores nigericin and valinomycin, before live imaging. The red horizontal bar is the mean and error bar is the s.d. **c**, Micro-dissected posterior PSM incubated with 20 µM BCECF ($n = 7$). Fluorescence intensities for excitation at 405 nm (blue) and 488 nm (green) are shown (left). In addition, the 488/405-nm ratio is shown (right). Scale bars, 100 µm. A, anterior; P, posterior. **d**, Fluorescence 488/405-nm ratios along the PSM. Each coloured line corresponds to an explant ($n = 7$ from two independent experiments). med, medial PSM; pos, posterior region. Two-sided, paired *t*-test. $^{**}P = 0.009$. **e**, **f**, Whole-mount in situ hybridization of 2-day-old chicken embryos cultured at different pH and hybridized with *MSGN1* (pH 5.3: $n = 4$, pH 7.2: $n = 3$ and pH 7.6: $n = 3$) (**e**) and *SAX1* (pH 5.3: $n = 6$, pH 7.2: $n = 4$ and pH 7.6: $n = 5$) (**f**). The ventral view shows the anterior region to the top. Scale bars, 100 µm.

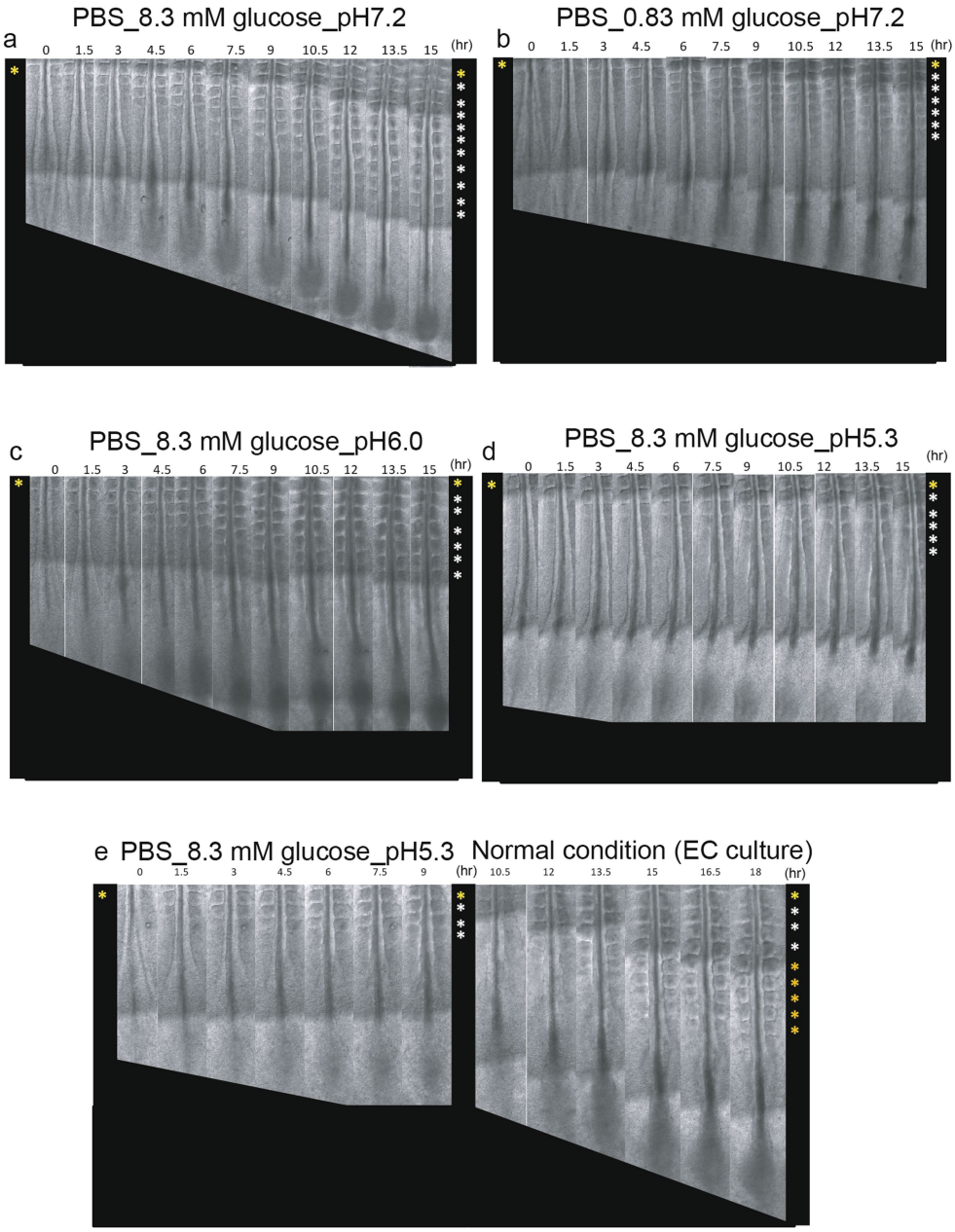

Extended Data Fig. 2 | Lowering the pHi can reversibly slow down embryo elongation. a, **b**, Snapshots of 2-day-old chicken embryos cultured in minimal medium at pH 7.2 with 8.3 mM ($n = 6$) glucose (**a**) or 0.83 mM glucose ($n = 3$) (**b**). **c**, **d**, Snapshots of 2-day-old chicken embryos cultured in minimal medium with 8.3 mM glucose in acidic conditions (pH 6.0: $n = 6$ (**c**) and pH 5.3: $n = 6$ (**d**)). **e**, Snapshots of a 2-day-old chicken embryo first cultured in minimal medium with 8.3 mM glucose at pH 5.3 showing the arrest of elongation after 9 h, and returned to control medium after 10.5 h showing the rescue of elongation ($n = 6$). All panels show bright-field micrographs of the posterior region of chicken embryos taken at 1.5-h intervals. Somites formed at the last time point are indicated by asterisks on the right. The yellow asterisks mark the last somite at the beginning of the culture and the white asterisks are the somites produced during the culture period. The ventral views show the anterior region to the top. Scale bars, 100 µm.

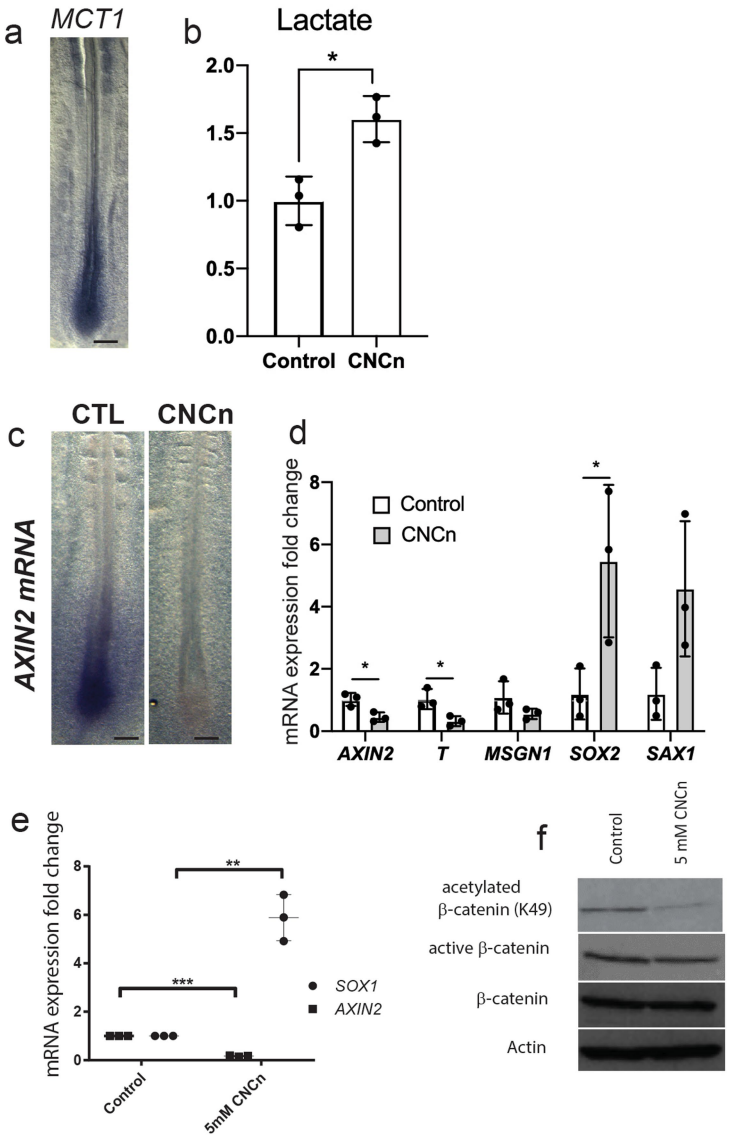

Extended Data Fig. 3 | Inhibiting lactate transporters downregulates WNT signalling. a, Whole-mount in situ hybridization of a 2-day-old chicken embryo hybridized with *MCT1* ($n = 4$). Scale bar, 100 µm. **b**, Comparison of lactate amounts in cellular extracts of the posterior region of 2-day-old chicken embryos cultured for 10 h in chemically defined medium with or without 5 mM CNCn ($n = 3$). Mean ± s.d. is shown. Two-sided, unpaired *t*-test, $P = 0.0292$. $^{*}P < 0.05$. **c**, Whole-mount in situ hybridization of 2-day-old chicken embryos cultured with 0 mM (control (CTL)) or 5 mM CNCn and hybridized with *AXIN2* (control: $n = 8$, 5 mM CNCn: $n = 7$). Scale bars, 100 µm. **d**, qPCR analysis of *MSGN1*, *SAX1*, *SOX2*, *T* and *AXIN2* expression in the posterior region of 2-day-old chicken embryos cultured with or without 5 mM CNCn ($n = 3$ for each gene). Data were normalized by control samples. Mean ± s.d. is shown. Two-sided, unpaired *t*-test. *AXIN2*: $P = 0.0197$, *T*: $P = 0.0270$, *SOX2*: $P = 0.0458$. $^{*}P < 0.05$. **e**, Comparison of *AXIN2* and *SOX1* mRNA expression in day 2 human iPS cells differentiated in vitro and cultured for 24 h in CL medium containing 5 mM CNCn or vehicle control (DMSO). $n = 3$ biological replicates. Mean ± s.d. is shown. Two-way ANOVA followed by Tukey's multiple comparisons test: $^{***}P = 0.0004$ and $^{**}P = 0.0067$. $n = 3$. **f**, Western blot analysis using anti-acetylated K49 β-catenin, anti-active β-catenin, anti-actin and anti-β-catenin of whole-cell extracts of 2-day-old chicken embryos cultured in chemically defined medium with 0 or 5 mM CNCn for 10 h ($n = 3$). For gel source data, see Supplementary Fig. 1.

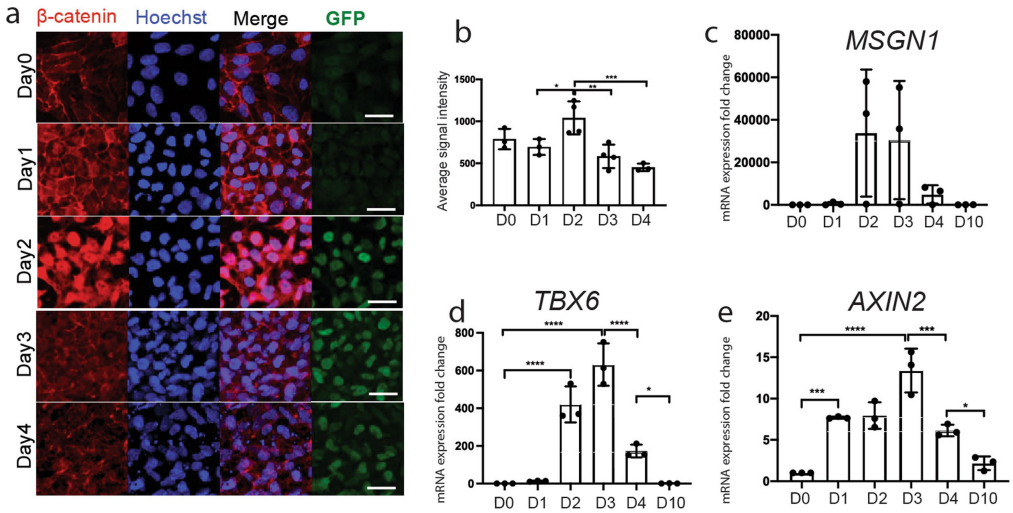

Extended Data Fig. 4 | Kinetics of WNT–β-catenin signalling during human iPS cell differentiation to the PSM. a, Immunohistochemistry showing the dynamic expression of β-catenin and Venus (YFP) proteins in human *MSGN1-Venus* iPS reporter cells differentiated to the PSM fate in vitro ($n = 3$). Hoechst labelling of the nuclei is shown in blue. Scale bars, 30 µm. **b**, Quantification of the intensity of nuclear localization of β-catenin shown in **a** using Fiji. Mean ± s.d. is shown (D0, D1 and D4: $n = 3$; D2 and D3: $n = 4$). One-way ANOVA followed by Tukey's multiple comparisons test: D1 versus D2: $P = 0.0411$, D2 versus D3: $P = 0.0038$, D2 versus D4: $P = 0.0009$. $^{*}P < 0.05$, $^{**}P < 0.01$ and $^{***}P < 0.001$. **c**–**e**, qPCR analysis comparing the expression level of *MSGN1* (**c**), *TBX6* (**d**) and *AXIN2* (**e**) of human iPS cells differentiating to the PSM fate in vitro. Values were normalized by the results of differentiation at D0. Mean ± s.d. is shown ($n = 3$). One-way ANOVA followed by Tukey's multiple comparisons test: *TBX6* D0 versus D2: $P < 0.0001$, D0 versus D3: $P < 0.0001$, D3 versus D4: $P < 0.0001$, D4 versus D10: $P = 0.0466$; *AXIN2* D0 versus D1: $P = 0.0006$, D0 versus D3: $P < 0.0001$, D3 versus D4: $P = 0.0003$, D4 versus D10: $P = 0.0318$ $^{*}P < 0.05$, $^{***}P < 0.001$ and $^{****}P < 0.0001$.

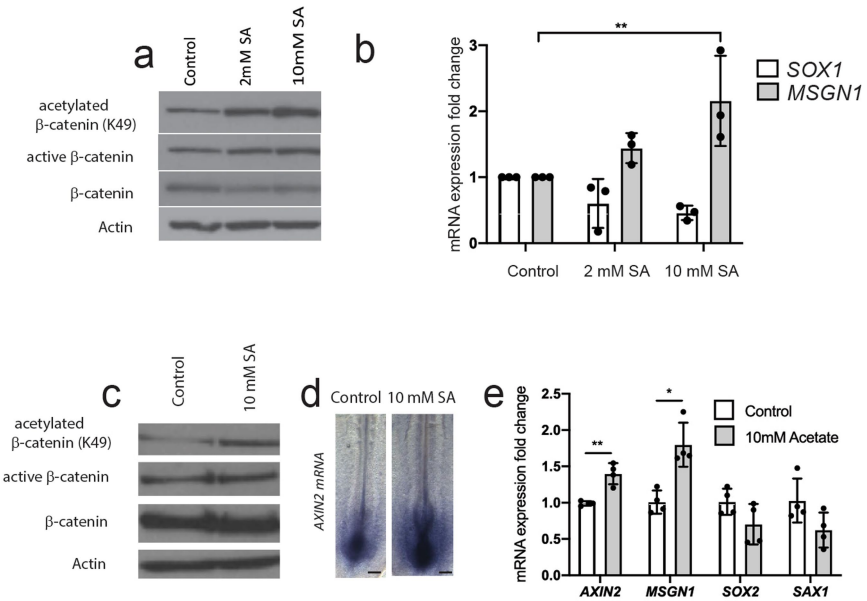

Extended Data Fig. 5 | Sodium acetate treatment increases WNT–β-catenin signalling in vivo and in vitro. a, Western blot analysis using anti-acetylated K49 β-catenin, anti-active β-catenin, anti-actin and anti-β-catenin. Whole-cell extracts of day 2 human iPS cells differentiated to PSM in vitro in CL medium and treated with sodium acetate (SA) for 24 h ($n = 3$). **b**, qPCR analysis of *SOX1* and *MSGN1* mRNA expression in day 2 human iPS cells differentiated to PSM in vitro and treated with SA in CL medium for 24 h. Mean ± s.d. is shown ($n = 3$). Two-way ANOVA followed by Tukey's multiple comparisons test. *MSGN1* control versus 10 mM SA: $P = 0.003$. $^{**}P < 0.01$. **c**, Western blot analysis using anti-acetylated K49 β-catenin, anti-active β-catenin, anti-actin and anti-β-catenin of whole-cell extracts of 2-day-old chicken embryos cultured in chemically defined medium with 0 or 10 mM SA for 10 h ($n = 3$). **d**, Whole-mount in situ hybridization of 2-day-old chicken embryos cultured with 0 or 10 mM SA and hybridized with *AXIN2* (control: $n = 5$ and 10 mM SA: $n = 7$). Scale bars, 100 µm. **e**, qPCR analysis of *AXIN2*, *MSGN1*, *SOX2* and *SAX1* expression in the posterior region of 2-day-old chicken embryos cultured with 0 or 10 mM SA. Data were normalized by control samples. Mean ± s.d. is shown ($n = 4$). Two-sided, unpaired *t*-test. *AXIN2*: $P = 0.0070$ and *MSGN1*: $P = 0.0298$. $^{*}P < 0.01$ and $^{**}P < 0.001$. For gel source data, see Supplementary Fig. 1.

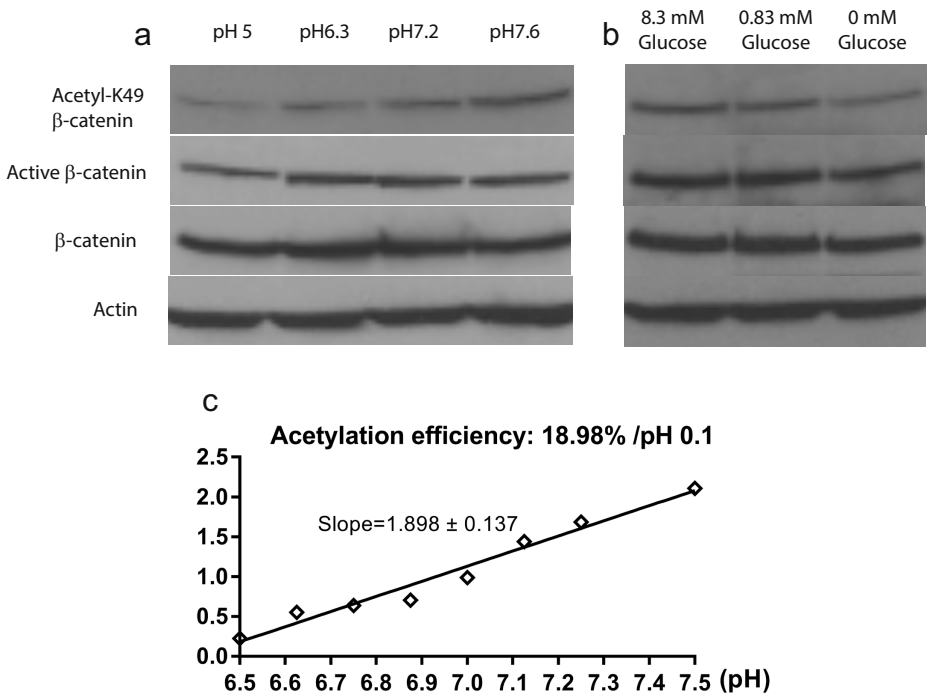

Extended Data Fig. 6 | β-Catenin acetylation depends on pHi and glycolytic activity. a, **b**, Western blot analysis using anti-acetylated K49 β-catenin, anti-active β-catenin, anti-actin and anti-β-catenin. Extracts of 2-day-old chicken embryos cultured in minimal medium with 8.3 mM glucose at various pH ($n = 3$ per condition) (**a**) or in minimal medium at pH 7.2 with various glucose concentrations ($n = 4$ per condition) (**b**). **c**, Quantification of acetylated lysine and β-catenin intensity in Fig. 3h using Fiji. The acetylation rate is calculated from the slope of the graph. $n = 2$ independent experiments. Linear approximation, mean ± s.d. of the slope. For gel source data, see Supplementary Fig. 1.

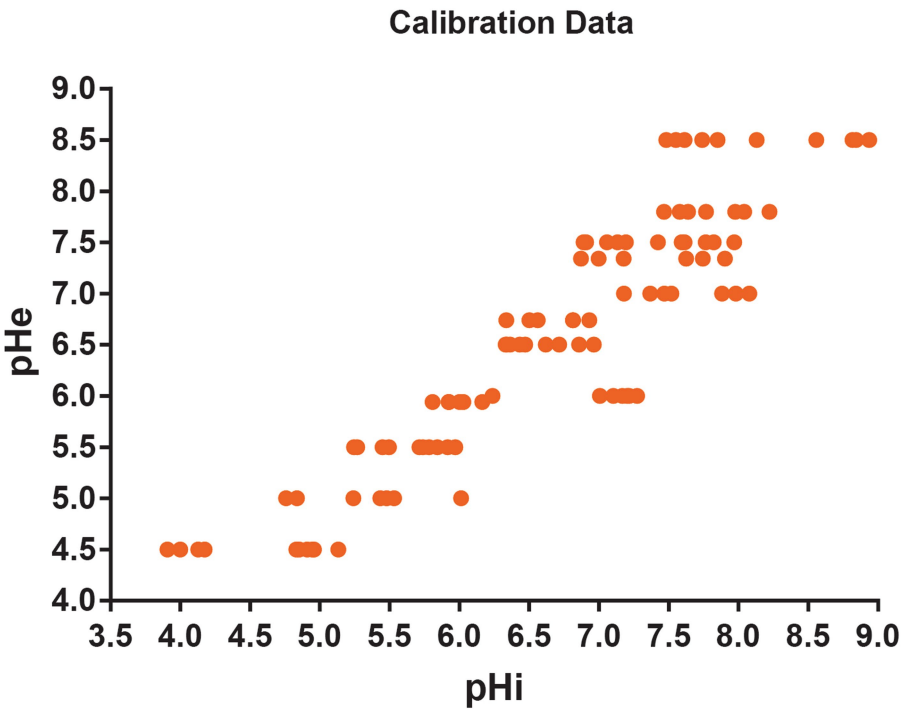

Extended Data Fig. 7 | Calibration curve used for quantifying pHi variations as a function of pHe in differentiating human iPS cells. Calibration curve obtained for the pH measurements in differentiated iPS cells in vitro using BCECF as described in the Methods. $n = 6$ independent experiments.

nature research

Corresponding author(s): Olivier Pourquie

Last updated by author(s): Mar 11, 2020

Reporting Summary

Nature Research wishes to improve the reproducibility of the work that we publish. This form provides structure for consistency and transparency in reporting. For further information on Nature Research policies, see Authors & Referees and the Editorial Policy Checklist.

Statistics

For all statistical analyses, confirm that the following items are present in the figure legend, table legend, main text, or Methods section.

n/a	Confirmed	
☐	☒	The exact sample size (*n*) for each experimental group/condition, given as a discrete number and unit of measurement
☐	☒	A statement on whether measurements were taken from distinct samples or whether the same sample was measured repeatedly
☐	☒	The statistical test(s) used AND whether they are one- or two-sided *Only common tests should be described solely by name; describe more complex techniques in the Methods section.*
☒	☐	A description of all covariates tested
☒	☐	A description of any assumptions or corrections, such as tests of normality and adjustment for multiple comparisons
☐	☒	A full description of the statistical parameters including central tendency (e.g. means) or other basic estimates (e.g. regression coefficient) AND variation (e.g. standard deviation) or associated estimates of uncertainty (e.g. confidence intervals)
☐	☒	For null hypothesis testing, the test statistic (e.g. *F*, *t*, *r*) with confidence intervals, effect sizes, degrees of freedom and *P* value noted *Give P values as exact values whenever suitable.*
☒	☐	For Bayesian analysis, information on the choice of priors and Markov chain Monte Carlo settings
☒	☐	For hierarchical and complex designs, identification of the appropriate level for tests and full reporting of outcomes
☒	☐	Estimates of effect sizes (e.g. Cohen's *d*, Pearson's *r*), indicating how they were calculated

Our web collection on statistics for biologists contains articles on many of the points above.

Software and code

Policy information about availability of computer code

Data collection	Wave version 2.6.1 (to collect and analyze seahorse data)
Data analysis	Graphpad Prism version 7, ImageJ (Fiji), GoFigure2 software, Custom made Matlab routines available at https://github.com/amichaut/pHanalysis

For manuscripts utilizing custom algorithms or software that are central to the research but not yet described in published literature, software must be made available to editors/reviewers. We strongly encourage code deposition in a community repository (e.g. GitHub). See the Nature Research guidelines for submitting code & software for further information.

Data

Policy information about availability of data

All manuscripts must include a data availability statement. This statement should provide the following information, where applicable:

- Accession codes, unique identifiers, or web links for publicly available datasets
- A list of figures that have associated raw data
- A description of any restrictions on data availability

All data generated or analyzed during this study are included in this published article (and its supplementary information files).

Field-specific reporting

Please select the one below that is the best fit for your research. If you are not sure, read the appropriate sections before making your selection.

☒ Life sciences ☐ Behavioural & social sciences ☐ Ecological, evolutionary & environmental sciences

Life sciences study design

All studies must disclose on these points even when the disclosure is negative.

Sample size	Sample sizes were not pre-determined. Rather, we ensured our sample sizes were sufficient by checking that inclusion of additional data points did not significantly change the variance (SD) of the data.
Data exclusions	We did not exclude data.
Replication	To ensure the reproducibility of our findings, we carried out all experiments several independent times (exact n for each experiment reported in the figure legends). Each independent experiment contained technical triplicates. We ensured that these independent datasets of similar size did not change the reported results.
Randomization	Randomization is not relevant as the same cell lines were used in all cases.
Blinding	Blinding is not applicable to data collection (see above). In the case of time-lapse imaging analysis, all labels were removed and individual microscopy files were analyzed blindly in ImageJ/MATLAB for all conditions tested.

Reporting for specific materials, systems and methods

We require information from authors about some types of materials, experimental systems and methods used in many studies. Here, indicate whether each material, system or method listed is relevant to your study. If you are not sure if a list item applies to your research, read the appropriate section before selecting a response.

Materials & experimental systems

n/a	Involved in the study
☐	☒ Antibodies
☐	☒ Eukaryotic cell lines
☒	☐ Palaeontology
☐	☒ Animals and other organisms
☒	☐ Human research participants
☒	☐ Clinical data

Methods

n/a	Involved in the study
☒	☐ ChIP-seq
☒	☐ Flow cytometry
☒	☐ MRI-based neuroimaging

Antibodies

Antibodies used	Goat anti-Rabbit IgG secondary antibody, Horseradish peroxidase (HRP) conjugate (Invitrogen, #31460, Lot SJ257972, 1:1000-1:10000), Goat anti-Mouse IgG secondary antibody, and HRP conjugate (Invitrogen, #31430, Lot SI259643, 1:1000-1:10000), Anti-actin antibody (Millipore, #MAB1501, Lot 2951837, 1:5000), Hoechst (Life technologies, #3570, Lot 1524924, 1:1000), Goat anti-Chicken IgY(H+L) Secondary antibody, Alexa fluoro 488 (Invitrogen, #A11039, Lot 1599396, 1:500), Goat anti-Rabbit IgY(H+L) Highly Cross Absorbed Secondary antibody, Alexa fluoro 594 (Invitrogen, #A11037, Lot 1745277, 1:500), Anti-β-catenin antibody (BD, #610153, Lot 2146908, 1:1000), Anti Acetyl-β-catenin (Lys49) antibody (Cell Signaling Technology, #9534S, Lot 2, 1:1000), Anti GAPDH antibody (abcam #ab125247, Lot gr285925-3, 1:1000), chicken anti-GFP antibody (invitrogen #ab13970, Lot gr3190550-6, 1:800), Anti laminB1 antibody (abcam, #ab16048, Lot 3210079-1, 1:5000), Anti-Active-β-catenin antibody (Millipore, #05-665,. Lot, 1:1000), Anti-acetyl Lysine antibody (cell signaling #9441, Lot, 1:1000)
Validation	All antibodies were validated by the suppliers and accurately represent expected expression patterns. -Actin: Anti-Actin Antibody, clone C4. Reliably and specifically detect actin using this Anti-Actin Antibody, clone C4. This highly published monoclonal antibody is validated for use in ELISA, IC, IF, IH, IH(P) & WB. Reactivity notes: To date, all animal species and cell types with an actin form react by indirect immunofluorescence or immunoblot, including plant actin. This mAb is also available as a fluorescent conjugate. (http://www.emdmillipore.com/US/en/product/Anti-Actin-Antibody-clone-C4,MM_NF-MAB1501?bd=1) -Hoechst: Invitrogen Hoechst 33342 nucleic acid stain is a popular cell-permeant nuclear counterstain that emits blue fluorescence when bound to dsDNA. This dye is often used to distinguish condensed pycnotic nuclei in apoptotic cells and for cell cycle studies in combination with BrdU. (https://www.thermofisher.com/jp/en/home/references/protocols/cell-and-tissue-analysis/protocols/hoechst-33342-imaging-protocol.html) -β-catenin: Reactivity Human (QC Testing) Mouse, Rat, Dog, Chicken (Tested in Development) , Application Western blot (Routinely Tested) Immunohistochemistry, Immunoprecipitation, Immunofluorescence (Tested During Development) (https://www.bdbiosciences.com/us/applications/research/stem-cell-research/cancer-research/human/purified-mouse-anti--catenin-14beta-catenin/p/610153) -Active-β-catenin: Anti-Active-β-Catenin (anti-ABC) Antibody, clone 8E7 is a well characterized Mouse Monoclonal Antibody. This highly published mAb also known as Anti-Catenin beta-1 readily detects beta-Catenin & has been validated in FC, ICC, IHC, IHC(P) & WB. Reactivity: Human, Mouse, Rat (http://www.emdmillipore.com/US/en/product/Anti-Active-Catenin-Anti-ABC-Antibody-clone-8E7,MM_NF-05-665?bd=1#) -LaminB1: Application; ICC/IF, IHC-Fr, WB, IHC-P, IHC – Wholemount, Reactivity; Mouse, Rat, Human, Pig, Xenopus laevis, Indian muntjac (https://www.abcam.co.jp/lamin-b1-antibody-nuclear-envelope-marker-ab16048.html)

-GAPDH: Application; WB, Dot blot, ELISA, Reactivity; Mouse, Rat, Rabbit, Chicken, Hamster, Human, Saccharomyces cerevisiae, Schizosaccharomyces pombe (https://www.abcam.co.jp/gapdh-antibody-ga1r-loading-control-ab125247.html)
-Acetylated Lysine: Application; Western, Immunoprecipitation, Immunohistochemistry, ChIP, IF, Flow Cytometry, ELISA- Peptide, Reactivity; Human, Mouse, Hamster, Monkey, Mink, Chicken, D. melanogaster, Xenopus, Zebrafish, Bovine, Dog, Pig, S. cerevisiae, C. elegans, Horse, All Species Expected (https://www.cellsignal.jp/products/primary-antibodies/acetylated-lysine-antibody/9441)
-Chicken anti-GFP: Application; IHC-P, WB, IHC - Wholemount, IHC-FrFl, ICC/IF, IHC-Fr, IHC-FoFr, Reactivity: Recombinant full length protein corresponding to GFP (https://www.abcam.co.jp/gfp-antibody-ab13970.html)
-Acetyl-β-Catenin (Lys49) : Specificity / Sensitivity: Acetyl-β-Catenin (Lys49) Antibody detects endogenous β-catenin only when acetylated at Lys49. Applications: WB. Species Reactivity: Human, Species predicted to react based on 100% sequence homology: Mouse, Rat, Pig (https://www.cellsignal.com/products/primary-antibodies/acetyl-b-catenin-lys49-antibody/9534)
-Acetyl Lysine antibody,Acetylated-Lysine Antibody detects proteins posttranslationally modified by acetylation on the epsilon-amine groups of lysine residues. Applications: WB, IP, IHC, IF, ChIP. Species Reactivity: all (Human, Mouse, Rat, Hamster, Monkey, Chicken) (https://www.cellsignal.jp/products/primary-antibodies/acetylated-lysine-antibody/9441).

Eukaryotic cell lines

Policy information about cell lines

Cell line source(s)	The human iPS NCRM1 line was obtained from RUCDR Infinite Biologics at Rutgers University. The mono-allelic mEGFP-tagged CTNNB1 WTC iPSC line was obtained from the Allen Cell Collection at the Coriell Institute. The MSGN1-RepV human iPS line was generated in the lab from the parental line 11a which was obtained from HSCI.
Authentication	Authentication was unnecessary due to the unique morphology of human iPS, as well as their unique differentiation potential.
Mycoplasma contamination	All cell lines tested negative for mycoplasma contamination.
Commonly misidentified lines (See ICLAC register)	No commonly misidentified cell lines were used.

Animals and other organisms

Policy information about studies involving animals; ARRIVE guidelines recommended for reporting animal research

Laboratory animals	We don't use the laboratory animals.
Wild animals	Fertilized chicken eggs were obtained from commercial sources.
Field-collected samples	The study did not involve samples collected from the field.
Ethics oversight	The office for protection from Research Risks (OPRR) has interpreted "live vertebrate animal" to apply to avians (e.g., chick embryos) only after hatching (http://grants.nih.gov/grants/olaw/references/ilar91.htm). All of the studies proposed in this project only concern early developmental stages (prior to 5 days of incubation), therefore no IACUC approved protocol is required.

Note that full information on the approval of the study protocol must also be provided in the manuscript.